



Published in final edited form as:

*J Pharm Sci.* 2014 May ; 103(5): 1375–1383. doi:10.1002/jps.23939.

## Structure and Activity of a New Low Molecular Weight Heparin Produced by Enzymatic Ultrafiltration

LI FU<sup>1,2</sup>, FUMING ZHANG<sup>3</sup>, GUOYUN LI<sup>2,6</sup>, AKIHIRO ONISHI<sup>2</sup>, UJJWAL BHASKAR<sup>3</sup>, PEILONG SUN<sup>1</sup>, and ROBERT J. LINHARDT<sup>2,3,4,5</sup>

<sup>1</sup>Department of Biotechnology, College of Biological & Environmental Engineering, Zhejiang University of Technology, Hangzhou, 310032, China

<sup>2</sup>Department of Chemistry and Chemical, Center for Biotechnology and Interdisciplinary Studies, Rensselaer Polytechnic Institute, Troy, New York 121806, USA

<sup>3</sup>Department of Chemical and Biological Engineering, Biology, Center for Biotechnology and Interdisciplinary Studies, Rensselaer Polytechnic Institute, Troy, New York 121806, USA

<sup>4</sup>Department of Biology, Center for Biotechnology and Interdisciplinary Studies, Rensselaer Polytechnic Institute, Troy, New York 121806, USA

<sup>5</sup>Department of Biomedical Engineering, Center for Biotechnology and Interdisciplinary Studies, Rensselaer Polytechnic Institute, Troy, New York 121806, USA

<sup>6</sup>College of Food Science and Technology, Ocean University of China, No.5, Yu Shan Road, Qingdao, Shandong, 266003, China

### Abstract

The standard process for preparing the low molecular weight heparin (LMWH) tinzaparin, through the partial enzymatic depolymerization of heparin, results in a reduced yield due to the formation of a high content of undesired disaccharides and tetrasaccharides. An enzymatic ultrafiltration reactor for LMWH preparation was developed to overcome this problem. The behavior, of the heparin oligosaccharides and polysaccharides using various membranes and conditions, was investigated to optimize this reactor. A novel product, LMWH-II, was produced from the controlled depolymerization of heparin using heparin lyase II in this optimized ultrafiltration reactor. Enzymatic ultrafiltration provides easy control and high yields (>80%) of LMWH-II. The molecular weight properties of LMWH-II were similar to other commercial LMWHs. The structure of LMWH-II closely matched heparin's core structural features. Most of the common process artifacts, present in many commercial LWMHs, were eliminated as demonstrated by 1D and 2D nuclear magnetic resonance spectroscopy. The antithrombin III and platelet factor-4 binding affinity of LMWH-II were comparable to commercial LMWHs, as was its *in vitro* anticoagulant activity.

## Keywords

Low molecular weight heparin; heparin lyase; ultrafiltration; nuclear magnetic resonance spectroscopy; liquid chromatography-mass spectrometry; surface plasmon resonance; anticoagulant; anti-Xa; anti-IIa

## INTRODUCTION

Heparin (also known as unfractionated heparin (UFH)) is a polysaccharide-based anticoagulant drug that was first introduced into clinical practice nearly 100 years ago.<sup>1</sup> Low molecular weight heparins (LMWHs), derived from UFH, were more recently introduced, nearly 35 years ago.<sup>1,2</sup> The need for heparin and LMWHs continues to increase as modern medical treatments and procedures, such as the treatment of deep vein thrombosis, postsurgical control of clots,<sup>3,4</sup> extracorporeal therapy (*i.e.*, kidney dialysis and heart-lung oxygenators), and the use of indwelling heparinized catheters and shunts, expand in first-world countries and are introduced in third-world countries.

The major repeating disaccharide unit of heparin is  $\alpha$ -L-IdoA2S(1 $\rightarrow$ 4)- $\alpha$ -D-GlcNS6S (where IdoA is idopyranosyluronic acid, S is sulfo, and GlcN is 2-deoxy, 2-amino glucopyranose), but the minor disaccharide units are also present with different structural and sulfation patterns that are integral to heparin's major therapeutic activity, the inhibition of coagulation cascade proteases, thrombin (factor IIa) and factor Xa. A well studied pentasaccharide sequence in heparin having the structure,  $\rightarrow$ 4)- $\alpha$ -D-GlcNAc6S(1 $\rightarrow$ 4)- $\beta$ -D-GlcA(1 $\rightarrow$ 4)- $\alpha$ -D-GlcNS3S6S(1 $\rightarrow$ 4)- $\alpha$ -L-Ido2S(1 $\rightarrow$ 4)- $\alpha$ -D-GlcNS6S(1 $\rightarrow$  (where GlcA is glucopyranosyluronic acid and Ac is acetyl) is critical to heparin's specific activation of the serine protease inhibitor antithrombin III (ATIII). Heparin is able to bind both ATIII and thrombin to afford a ternary complex, inactivating thrombin and thus preventing fibrin clot formation. FXa does not interact directly with heparin but is instead inhibited by heparin-ATIII binary complex. The inactivation of thrombin by ATIII requires the longer heparin chains (>15 saccharide units) common to UFH, while small heparin chains (from 5 to 15 saccharide units) common to LMWH, are capable of binding only ATIII, inactivating factor Xa. Thus, LMWHs are considered factor Xa selective anticoagulant/antithrombotic drugs.<sup>1,5</sup>

The major physiologic role of platelet factor-4 (PF4), which is released from the alpha-granules of activated platelets, is to bind and neutralize heparin and heparan sulfate on the endothelial surface of blood vessels, thereby inhibiting local ATIII activation and promoting coagulation. The heparin-PF4 complex is the antigen in heparin-induced thrombocytopenia (HIT), an idiosyncratic autoimmune reaction to the administration of the anticoagulant heparin. LMWHs have a lower binding affinity for PF4 than does heparin, which both improve their anticoagulant activity and reduce their incidence of HIT.<sup>6,7</sup> Finally, the enhanced *subcutaneous* bioavailability and improved pharmacodynamics of LMWHs have increased the clinical use of these anticoagulants in recent years.<sup>1,8</sup>

Currently the commercial preparation of LMWHs from UFH includes the controlled chemical depolymerization of heparin by peroxidative cleavage, nitrous acid cleavage, and chemical  $\beta$ -elimination (Fig 1. Upper panel, II to III). These chemical methods result in

process artifacts including 2,6-anhydromannitol (Fig. 1, lower panel, structure 1), epoxide (Fig. 1, lower panel, structure 2), 1,6-anhydroglucopyranose (Fig. 1, lower panel, structure 3) and 1,6-anhydromannopyranose (Fig. 1, lower panel, structure 4), as a result of harsh reaction conditions that are used in their preparation.<sup>9,10</sup> In contrast, enzymatic depolymerization, a much milder approach, has also been used to make LMWH. Heparin lyase I, isolated from *Flavobacterium heparinum*, is most commonly used to enzymatically depolymerize heparin (Fig. 1, upper panel, II to I).<sup>8,11,12,13</sup> Previous studies, however, demonstrate that while both heparin lyase I and II can cleave  $\rightarrow 4$ - $\alpha$ -D-GlcNS6S(1 $\rightarrow$ 4)- $\alpha$ -L-IdoA2S(1 $\rightarrow$ ) linkage, heparin lyase I is highly selective for  $\rightarrow 4$ - $\alpha$ -D-GlcNS3S6S(1 $\rightarrow$ 4)- $\alpha$ -L-IdoA2S(1 $\rightarrow$ ) and heparin lyase II has selectivity for  $\rightarrow 4$ - $\alpha$ -D-GlcNS6S(1 $\rightarrow$ 4)- $\alpha$ -L-IdoA(1 $\rightarrow$ ).<sup>14,15</sup>

Heparin lyases can be used under mild conditions (room temperature at physiologic pH) to afford LMWHs (Fig. 1 Panel I) with fewer process artifacts generated through side-reactions. However, enzymatic depolymerization without chain length control can easily result in the over-digestion of heparin, converting an active LMWH into smaller chains without bioactivity, such as disaccharides and tetrasaccharides. Moreover, the heparin lyases, particularly heparin lyase I, are known to selectively act at linkages present within the ATIII-pentasaccharide binding site<sup>15</sup> making the loss of anticoagulant activity particularly hard to control. Thus, the efficient separation of bioactive oligosaccharides throughout the reaction, protecting them from full depolymerization, is crucial to obtain active LMWH in high-yield. In this report, we developed an enzymatic ultrafiltration reactor for LMWH preparation employing mild heparin lyase-catalyzed depolymerization conditions with simultaneous product separation. The chemical structure and *in vitro* bioactivity of the resulting LMWH products were characterized.

## MATERIALS AND METHODS

### Materials

Unfractionated porcine heparin (UFH) sodium salt 200 U/mg was from Celsus (Cincinnati, OH) and bovine heparin sodium salt 150 U/mg was from Sigma Chemical Co. (St. Louis, MO). Recombinant *Flavobacterium heparinum* heparin lyase I and II were expressed in our laboratory using *Escherichia coli* strains, provided by Professor Jian Liu, University of North Carolina, College of Pharmacy, Chapel Hill, NC).<sup>22</sup> Heparin oligosaccharides, from hexasaccharide to icosasaccharide, were used as calibrants for molecular weight determination by size-exclusion chromatography (SEC) and were purchased from Iduron (Manchester, UK). Unsaturated heparan sulfate-heparin disaccharide standards (0S, UA-GlcNAc; NS, UA-GlcNS; 6S, UA-GlcNAc6S; 2S, UA2S-GlcNAc; 2SNS, UA2S-GlcNS; NS6S, UA-GlcNS6S; 2S6S, UA2SGlcNAc6S; and TriS, UA2S-GlcNS6S, where UA is deoxy- $\alpha$ -L-threo-hex-4-enopyranosyl uronic acid) were obtained from Seikagaku Corporation (Chuo-ku, Tokyo, Japan). ATIII and PF4 were from Aniar (West Chester, Ohio).

## Ultrafiltration Behavior of Heparin Oligosaccharides in Various Membranes

Ultrafiltration behavior of heparin oligosaccharides was tested using four different molecular weight cut-off (MWCO) membranes, 3, 5, 10, and 30 kDa. Bovine lung heparin partially digested with heparin lyase I<sup>23</sup> (10 mg in 1 ml distilled water) was filtered through (10,000 × g at 22 °C) an Amicon centrifugal filter with a 30-kDa MWCO membrane (Millipore, Billerica, MA, USA). The retained fraction was collected (30KT) and the permeate fraction was next filtered through 10-kDa MWCO membrane, the retained (10KT) and permeate fractions were again collected. In the same way, 5KT and 3KT fractions were collected using 5-kDa and 3-kDa membranes, respectively. The final permeate fraction (3KP) obtained using a 3-kDa MWCO membrane was also collected.

Defined heparin derived oligosaccharides<sup>24</sup> each of a different degree of polymerization (dp)8 (MW ~ 2653 Da), dp10 (MW ~ 3317 Da) and dp12 (MW ~ 3980 Da) (1 mg each), were individually filtered through 3-kDa, 5-kDa and 10-kDa MWCO membranes. All of the retained and permeate fractions of dp8, dp10 and dp12 were collected and lyophilized for carbazole assay<sup>25</sup> and polyacrylamide gel electrophoresis (PAGE) analysis.<sup>23</sup>

## Enzymatic Ultrafiltration Reactor

The enzymatic ultrafiltration reactor set up consisted of a 50 mL stirred ultrafiltration cell unit (Model 8050, Millipore, Billerica, MA) connected with a pressure-controllable nitrogen cylinder and a magnetic stirrer. Unfractionated porcine heparin (100 mg) was dissolved in 25 mL of reaction buffer (40 mM ammonium acetate and 3 mM calcium acetate (pH 7.0)). The reaction was initiated by adding heparin lyase I or heparin lyase II into the ultrafiltration reactor equipped with 10-KDa membrane (Millipore, Billerica, MA) under 2 or 20 psi N<sub>2</sub> pressure (as controlled by a nitrogen cylinder regulator) at room temperature (22 °C). When the reaction volume was reduced to 5 mL the pressure was released and the reactor was refilled by adding 15 mL of reaction buffer before resuming filtration at the same pressure. The permeate fraction was monitored using ultraviolet spectrophotometry at 232 nm. All of the permeate fractions were pooled, concentrated and desalted by dialysis with 3-kDa MWCO membrane. The final desalted product (LWMH) was lyophilized for further quantification and for structure/activity analysis. Different amounts of heparin lyase I or II, and different operating pressures were tested to optimize product yields.

## SEC of Heparin for Molecular Weight Measurement

Size-exclusion chromatography was performed using TSK-GEL G3000PWxI size-exclusion column (Tosoh Corporation, Minato-Ku, Tokyo, Japan) with a sample injection volume of 20 µL and a flow rate of 0.6 mL/min on an apparatus composed of a Shimadzu LC-10Ai pump, a Shimadzu CBM-20A controller, and a Shimadzu RID-10A refractive index detector (Shimadzu, Kyoto, Japan). The mobile phase consisted of 0.1 M aqueous NaNO<sub>3</sub>. The column was maintained at 40 °C during the chromatography with an Eppendorf column heater (Eppendorf, Hamburg, Germany). The SEC chromatograms were recorded with the LC solution version 1.25 software (Shimadzu, Kyoto, Japan) and analyzed with its “GPC Postrun” function. The molecular weight determination was carried out as previously reported.<sup>16</sup>

## Polyacrylamide Electrophoresis

Heparin oligosaccharide samples were analyzed by PAGE using 0.75 mm × 6.8 cm × 8.6 cm mini-gels cast from 22% resolving gel monomer solution and 5% stacking gel monomer solution, and LMWHs and UFH were analyzed by PAGE using 0.75 mm × 6.8 cm × 8.6 cm mini-gels cast from 15% resolving gel monomer solution and 5% stacking gel monomer solution. Each sample of 10 µg was loaded into the gel, purified dp10 and partially digested bovine lung heparin<sup>23</sup> were used as molecular markers. The mini-gels were subjected to electrophoresis at a constant 200 V for 110 min and visualized with 0.5% (w/v) alcian blue in 2% (v/v) aqueous acetic acid solution.<sup>23</sup>

## NMR Analysis

LMWH samples were analyzed by <sup>1</sup>H, <sup>13</sup>C nuclear magnetic resonance (NMR), and two-dimensional NMR spectroscopy. Heteronuclear single-quantum coherence (HSQC), proton–proton correlation spectroscopy (HHCOSY) and total correlation spectroscopy (TOCSY) were used to characterize their structures.<sup>2,17</sup> All NMR experiments were performed on Bruker Advance II 600 MHz spectrometer (Bruker Bio Spin, Billerica, MA) with Topspin 2.1.6 software (Bruker). Samples were each dissolved in 0.5 mL <sup>2</sup>H<sub>2</sub>O (99.996 %, Sigma Chemical Company) and freeze-dried repeatedly to remove the exchangeable protons. The samples were redissolved in 0.4 mL <sup>2</sup>H<sub>2</sub>O and transferred to NMR microtubes (outside diameter, 5 mm, Norell (Norell, Landisville, NJ)). The conditions for one-dimensional <sup>1</sup>H-NMR spectra were as follows: wobble sweep width of 12.3 kHz, acquisition time of 2.66 s, and relaxation delay of 8.00 s. Temperature was 298 K. The conditions for two-dimensional HSQC spectra were as follows: 32 scans, sweep width of 6.15 kHz, acquisition time of 0.33 s, and relaxation delay of 0.90 s. The conditions for two-dimensional HHCOSY spectra were as follows: 16 scans, sweep width of 7.46 kHz, acquisition time of 0.28 s, and relaxation delay of 1.50 s.<sup>16</sup>

## Enzymatic Digestion for Disaccharide Analysis and Tetrasaccharide Mapping

For disaccharides analysis, the heparin lyase I, II, and III (10 mU each) in 5 µL of 25 mM tris (hydroxymethyl) amino methane (Tris), 500 mM NaCl, 300 mM imidazole buffer (pH 7.4) were added to 10 µg LMWH sample in 25 µL of distilled water and incubated at 35 °C for 10 h to completely degrade the heparin sample. The products were recovered by centrifugal filtration using an YM-10 microconcentrator (Millipore, Billerica, MA), and the heparin disaccharides were recovered in permeate and freeze-dried. The resulting heparin disaccharides were dissolved in water to concentration of 50–100 ng/2 µL for liquid chromatography (LC)-mass spectrometric (MS) analysis.<sup>8,18</sup> For tetrasaccharides analysis, the heparin lyase II (40 mU in 20 µL of 25 mM Tris, 500 mM NaCl, 300 mM imidazole buffer (pH 7.4)) was added to 50–100 µg heparin sample in 40 µL of distilled water and incubated at 35 °C for 10 h. The degraded production was freeze-dried for subsequent LC-MS analysis.<sup>8</sup>

## Disaccharide Analysis and Tetrasaccharide Mapping Using LC-MS

Liquid chromatography–mass spectrometry (LC-MS) analyses were performed on an Agilent 1200 LC/MSD instrument (Agilent Technologies, Inc. Wilmington, DE) equipped

with a 6300 ion trap and a binary pump followed by a UV detector equipped with a high-pressure cell.<sup>19</sup> The column used was a Poroshell 120 C18 column (2.1 × 100 mm, 2.7 μm, Agilent, USA). Eluent A was water/acetonitrile (85:15) v/v, and eluent B was water/acetonitrile (35:65) v/v. Both eluents contained 12 mM TrBA and 38 mM ammonium acetate with pH adjusted to 6.5 with acetic acid. For disaccharides analysis, a gradient of solution A for 5 min followed by a linear gradient from 5 to 15 min (0–40% solution B) was used at flow rate of 150 μL/min.

For tetrasaccharide analysis,<sup>8</sup> a gradient of solution A for 2 min followed by a linear gradient from 2 to 40 min (0%–30% solution B) was used at a flow rate of 150 μL/min. The column effluent entered the source of the electrospray ionization (ESI)–MS for continuous detection by MS. The electrospray interface was set in the negative ionization mode with a skimmer potential of –40.0 V, a capillary exit of –40.0 V, and a source temperature of 350 °C, to obtain the maximum abundance of the ions in a full-scan spectrum (200–1500 Da). Nitrogen (8 L/min, 40 psi) was used as a drying and nebulizing gas.

### Surface Plasmon Resonance Analysis

Biotinylated heparin prepared from Celsus heparin was immobilized to sensor chip SA (streptavidin) (GE Healthcare, Uppsala, Sweden) based on the manufacturer's protocol. Surface plasmon resonance (SPR) measurements were performed on a BIAcore 3000 (GE Healthcare, Uppsala, Sweden) operated using the version software. Solution competition studies between surface heparin and soluble different LMWHs to measure IC<sub>50</sub> were performed using SPR.<sup>5</sup> AT III (250 nM) mixed with different of concentrations (0, 9.4, 18.8, 37.5, 75, 150 to 300 μg/mL) of heparin and PF4 mixed with different of concentrations (0, 3.2, 6.3 12.5 and 25.0 μg/mL) of heparin in HBS-EP buffer (10 mM of 2-[4-(2-hydroxyethyl)piperazin-1-yl]ethanesulfonic acid (HEPES), 150 mM sodium chloride, 3 mM ethylenediaminetetraacetic acid (EDTA), 0.005% polysorbate surfactant P20, pH 7.4) (GE Healthcare, Uppsala, Sweden) were injected over heparin chip at a flow rate of 30 μL/min, respectively. After each run, the chip was regenerated with 1 min injections each of glycine pH 2.5, 2M NaCl and HBS-EP buffer. For each set of competition experiments on SPR, a control experiment (only protein without heparin) was performed to make sure the surface was completely regenerated and that the results obtained between runs were comparable.

### Anti-FIIa and Anti-FXa Assays

The anti-Xa and anti-IIa activities of LMWHs were determined using BIOPHEN Heparin Anti-Xa (2 stage) and Anti-IIa (2 stage) kits (Aniara, West Chester, Ohio). Human ATIII 40 mU in 80 μL R1 buffer (Tris 0.05 M, NaCl 0.175 M, EDTA 0.0075 M, at pH 8.40 containing PEG at 0.1 %, and sodium azide as preservative) for anti-Xa assay and human ATIII 10 mU in 80 μL R2 buffer (Tris 0.05 M, NaCl 0.175 M, EDTA 0.0075 M, at pH 8.40 containing bovine serum albumin (BSA) at 0.2 %, and sodium azide as preservative) mixed with different masses of heparin (range from 0, 5, 10, 15 and 20 ng) were incubated for 2 min at 37 °C. Then, purified bovine factor Xa (320 ng in 40 μL R1 buffer) or purified human thrombin (960 mU in 40 μL in R2 buffer) pre-incubated at 37 °C were added and incubated for 2 min before the addition of chromogenic substrate specific for factor Xa (CS-01(65), 1.2 mM, 40 μL) or the chromogenic substrate specific for thrombin (CS-01(38), 1.25 mM,

40  $\mu$ L). The reaction mixture was incubated at 37 °C for 2 min for anti-Xa assay and 1 min for anti-IIa assay and then stopped with citric acid (20 mg/mL, 80  $\mu$ L). The absorbance was measured at 405 nm. Anti-Xa and anti-IIa activities were calculated using a standard curve of different concentrations of heparin (0–1 U/mL).

## Results and Discussion

### Behavior of Heparin Oligosaccharides in Membrane Filtration

Most commercial ultrafiltration membranes with controlled MWCO are calibrated based on spherically shaped analytes, such as globular proteins. Pore size is a critical parameter for the development of the ultrafiltration reactor. Therefore, the behavior of linear, rodlike heparin oligosaccharides was investigated using commercial membranes having various pore sizes. PAGE analysis clearly demonstrated that oligosaccharides smaller than dp10 (MW ~ 2687 Da) were nearly absent in 30KT and 10KT fractions (Fig. 2 Panel **b**). Moreover, oligosaccharides prominent in these fractions were relatively long heparin chains of molecular weight > 5500 Da. In contrast, the 5KT and 3KT fractions contained oligosaccharides of shorter chain lengths having molecular weights between 1000 and 6400 Da. Disaccharides (dp2, MW ~ 663 Da) and tetrasaccharides (dp4, MW ~ 1326 Da) were the major oligosaccharides found in the 3KP fraction. The ultrafiltration experiments on purified dp8, dp10 and dp12 oligosaccharides using 3-kDa, 5-kDa and 10-kDa MWCO membrane provided the recovery yields of these oligosaccharides as a function of membrane pore size (Table 1). The recovery was reduced as the molecular size of oligosaccharide became larger for each membrane tested and the recovery yield of the oligosaccharides tested all increased as the membrane pore size increased. Based on the molecular weight of the expected for a typical LMWH product (3,000–8,000 Da), a 10-kDa membrane was selected for optimal product recovery by enzymatic ultrafiltration.

### Heparin Enzymatic Ultrafiltration

Six different enzymatic ultrafiltration reactions were examined, two of which afforded LMWH-I and LMWH-II (Table 2). Relatively high pressure (20 psi) and a 10-kDa membrane afforded the best product recoveries of over 80% (determined by carbazole assay,<sup>25</sup> based on a linear standard curve  $y = 0.0184x + 0.1132$ ,  $r^2 = 0.99$ ) with reactions of 2 h at room temperature. These results suggest that enzymatic ultrafiltration offers a scalable alternative for the preparation of LMWH. The molecular weight data obtained on UFH, commercial LMWHs, LMWH-I, and LMWH-II, showed that LMWH-I and LMWH-II had molecular weight properties comparable with commercial LMWHs (Table 3). However, LMWH-I showed higher polydispersity as a result of a large portion of long chain product (Table 3, Fig. 2 Panel **a** and Panel **c**). In contrast, LMWH-II was comparable to commercial LMWHs on the basis of both average molecular weight and polydispersity and contained fewer long chain fractions (Table 3, Fig. 2 Panel **a** and Panel **c**). Thus, based on the molecular weight analyses, our focus turned to LMWH-II for further characterization.

### NMR Analysis

1D <sup>1</sup>H-NMR and 2D HHCOSY, TOCSY and HSQC NMR were carried out to characterize the structure of LMWH-II. The 1D <sup>1</sup>H-NMR spectra of Enoxaparin and UFH looked quite

similar, except the UA unit (Peak a, Fig. 3 panel a) formed from the chemical depolymerization. In LMWH-II, calcium induced chemical shifts of I<sub>2S</sub> protons at H1 and H5 were observed in both 1D <sup>1</sup>H-NMR (Fig. 3 Panel a) and 2D HSQC spectra (Fig. 3 Panel b and c).<sup>25</sup> This is not surprising as calcium was in the buffer used to prepare LMWH-II. Other peaks of LMWH-II in <sup>1</sup>H-NMR spectra looked similar to that of commercial LMWH and UFH. The anomeric signals of the reducing and non-reducing ends in LMWH-II from the cleaved →4)GlcNS6S(1→4)IdoA2S(1→ and →4)GlcNS6S(1→4)IdoA(1→ linkages (Fig. 1 Panel I) were all found in HSQC spectra (Fig. 3 Panel b), other internal saccharide signals for LMWH-II could be fully assigned from the HHCOSY, TCOSY and HSQC spectra (Fig 4 Panel a and c). Signals from the side-products (process artifacts) of chemical β-eliminative depolymerization in commercial LMWH were hidden behind the major heparin signals so were invisible in 1D<sup>1</sup>H-NMR, however, in 2D HSQC spectra, these process artifacts can be clearly seen. The UA<sub>2S</sub> and UA<sub>2OH</sub> signals, overlapped HSQC spectra of LMWH-II and in Enoxaparin, the 1,6-anhydro-glucopyranose (cross-peak C1, Fig. 3 Panel b and Fig. 1, lower panel structure 3), 1,6-anhydro-mannopyranose (cross peak C2, Fig. 3 Panel b and Fig. 1, lower panel structure 4) and epoxide from alkaline treatment of I<sub>2S</sub> (Fig. 1, lower panel structure 2) were found in Enoxaparin. By contrast, none of these process impurities were observed in LMWH-II. The 2,5-anhydromannitol residue (Fig. 1, lower panel structure 1), having the 3.9 to 4.3 ppm proton and 80–90 ppm carbon cross-peaks,<sup>10</sup> was also not present in LMWH-II.

### Disaccharide Analysis and Tetrasaccharide Mapping

Heparin can be nearly completely converted to disaccharides through its treatment with heparin lyases I, II, and III. Although disaccharide analyses of heparin have been previously published,<sup>17, 18</sup> the results of these analyses are dependent on the analytical method used and inter-lab variation can be high. In the current study, the disaccharide analysis of heparin, LMWH-II and Enoxaparin were performed back-to-back in triplicate (Table 4). Since both LMWH-II and Enoxaparin were prepared from porcine-derived UFH, their disaccharide composition were similar. A notable exception was the level of TriS, which is enriched in LMWH-II and the level of 6S and NS6S, which are diminished in LMWH-II. These subtle changes in disaccharide composition comes from the preferential cleavage of heparin lyase II at sites containing these disaccharide sequences resulting in their presence in disaccharides and tetrasaccharide products eliminated by enzymatic ultrafiltration.

When heparin or LMWH is exhaustively treated with heparin lyase I, II and III in addition to the formation of disaccharides, some lyase-resistant tetrasaccharides are also formed (Fig. 4 Panel a, b and c) because of the presence of 3-*O*-sulfo containing glucosamine residues.<sup>18</sup> There are three major types of these heparin lyase II-resistant tetrasaccharides (T1-T3) as previously shown (Table 5).<sup>16</sup> Their molecular ratio provides a fingerprint of the heparin from which they are derived as well as an insight into the structural diversity of the AT-binding pentasaccharide sequence within heparin. Using tetrasaccharide standards,<sup>18</sup> a standard curve was constructed to calculate the relative distribution of these sites. Since LMWH-II and Enoxaparin are both derived from UFH prepared from porcine intestinal mucosa, the percentages of three tetrasaccharides were present at the similar levels (Fig. 4 Panel d). In commercial LMWH, an unexpected peak appeared between T2 and T3



tetrasaccharides peaks in extracted ion chromatography (Fig 5 Panel **b**). We believe that this peak is associated with tetrasaccharide side-products (process artifacts, see Fig. 1, lower panel) formed under the harsh chemical reaction conditions used to prepare Enoxaparin.

### Surface Plasmon Resonance Analysis

High ATIII affinity and low PF4-binding affinity are critical for the clinical utility of a LMWH. Previously we described the application of a competitive SPR binding assay for heparin.<sup>16</sup> Using SPR, solution/surface competition experiments were performed to determine the relative binding affinity of different heparins to ATIII and PF4. ATIII (500 nM) or PF4 (25 nM) were mixed with different concentrations of heparin in HBS-EP buffer were injected over heparin chip. Once the active binding sites on ATIII molecules were occupied by heparin in the solution, the binding of ATIII or PF4 to the surface-immobilized heparin is prevented, resulting in a reduction in SPR signal (Fig. 5 Panel **a** and **b**). The IC<sub>50</sub> values (concentration of competing analyte resulting in a 50% decrease in response units) were calculated from the plots (normalized ATIII or PF4 binding signal *versus* heparin concentration in solution). ATIII-binding affinity of heparin is dependent on the presence of an ATIII binding site structure within a heparin chain.<sup>1</sup> The calculated ATIII IC<sub>50</sub> value of LMWH-II was comparable to Enoxaparin (Fig. 5 panel c). The decrease of ATIII-binding affinity of LMWH-II compared to UFH is probably caused by the loss of a small number of ATII binding sites during the enzymatic depolymerization. PF4-binding affinity is dependent on the molecular weight of the heparin product being tested.<sup>28</sup> Thus, as expected, LMWH-II showed significantly lower PF4-binding compared to UFH but higher than that of than that of Enoxaparin (Fig. 5 panel d).

### Anti-Xa and Anti-IIa activities

The anti-Xa and anti-IIa activities of LMWH-II were next measured to investigate the anticoagulant activity properties of LMWH-II produced by enzymatic ultrafiltration (Table 6). As expected, UFH shows identical anti-Xa and anti-IIa activity with an anti-Xa/anti-IIa ratio of 1 (Table 6). The anti-Xa and anti-IIa activities of Enoxaparin were similar to the values reported in other recent publications.<sup>9, 21</sup> The anti-Xa/anti-IIa ratio of LMWH-II was 2.74 is within the range of values for other commercial LMWHs (2.38–4.10).<sup>21</sup>

### Conclusion

In the current study enzymatic ultrafiltration is used to obtain an 80% yield of LMWH-II in 2 h at room temperature. This is an improvement over the reported product recoveries in other recent investigations.<sup>21,27</sup> Economic considerations are critical in the preparation of LMWH, like any other commercial product. Although photochemical preparation of LMWHs can result in up to 93% yields, this approach requires 12 h and is difficult to scale.<sup>9</sup> Mild enzymatic depolymerization may be an ideal approach to produce LMWH because it is scalable, affords high recoveries of product and avoids the formation of product artifacts that are common in harsh chemical processes. The use of ultrafiltration in an enzymatic process promotes the recovery of primarily active chains providing good process control on product activity. Activity analysis and tetrasaccharide mapping also demonstrates that enzymatic ultrafiltration protect the crucial active ATIII-binding pentasaccharide. Further studies will

be required to access the *in vivo* biological activities and pharmacological efficacy of LMWH-II and to examine process scale-up.

## Acknowledgments

This work was supported by grants from the National Institutes of Health HL101721 and HL096972.

## References

1. Linhardt RJ. Heparin: Structure and activity. *J Med Chem.* 2003; 46:51–2554.
2. Guerrini M, Zhang Z, Shriver Z, Naggi A, Masuko S, Langer R, Casu B, Linhardt RJ, Torri G, Sasisekharan R. Orthogonal analytical approaches to detect potential contaminants in heparin. *Proc Nat AcadSci USA.* 2009; 106:16956–16961.
3. Weintraub AY, Sheiner E. Anticoagulant therapy and thromboprophylaxis in patients with thrombophilia. *Arch GynecolObstet.* 2007; 276:567–571.
4. Bick RL, Frenkel EP, Walenga J, Fareed J, Hoppensteadt DA. Unfractionated heparin, low molecular weight heparins, and pentasaccharide: basic mechanism of actions, pharmacology, and clinical use. *Hematol OncolClin North Am.* 2005; 19:1–51.
5. Beaudet J, Weyers A, Solakyildirim K, Yang B, Takieddin M, Mousa S, Zhang F, Linhardt RJ. Impact of autoclave sterilization on the activity and structure of formulated heparin. *J Pharm Sci.* 2011; 100:3396–3404. [PubMed: 21416466]
6. Eisman R, Surrey S, Ramachandran B, Schwartz E, Poncz M. Structural and functional comparison of the genes for human platelet factor 4 and PF4alt. *Blood.* 1990; 76:336–344. [PubMed: 1695112]
7. Warkentin TE. Drug-induced immune-mediated thrombocytopenia from purpura to thrombosis. *N Engl J Med.* 2007; 356:891–893. [PubMed: 17329695]
8. Xiao Z, Tappen BR, Mellisa LY, Zhao W, Canova LP, Guan H, Linhardt RJ. Heparin mapping using heparin lyase and the generation of a novel low molecular weight heparin. *J Med Chem.* 2011a; 54:603–610. [PubMed: 21166465]
9. Higashi K, Hosoyama S, Ohno A, Masuko S, Yang B, Sterner E, Wang Z, Linhardt RJ, Toida T. Photochemical preparation of a novel molecular weight heparin. *CarbohydPolym.* 2012; 87:1737–1743.
10. Keire DA, Buhse LF, Al-Hakim A. Characterization of currently marketed heparin products: composition analysis by 2D-NMR. *Anal Methods.* 2013; 5:2984–2994.
11. Yang VC, Linhardt RJ, Bernstein H, Cooney CL, Langer R. Purification and characterization of heparinase from *Flavobacterium heparinum*. *J Biol Chem.* 1985; 260:1849–1857. [PubMed: 3968088]
12. Lohse DL, Linhardt RJ. Purification and characterization of heparin lyases from *Flavobacterium heparinum*. *J Biol Chem.* 1992; 267:24347–24355. [PubMed: 1332952]
13. Linhardt RJ, Galliher PM, Cooney CL. Polysaccharide lyases. *ApplBiochemBiotechnol.* 1986; 12:135–177.
14. Toida T, Hileman RE, Smith AE, Vlahova PI, Linhardt RJ. Enzymatic preparation of heparin oligosaccharides containing antithrombin III binding sites. *J Biol Chem.* 1996; 271:32040–32047. [PubMed: 8943254]
15. Xiao Z, Zhao W, Yang B, Zhang Z, Guan H, Linhardt RJ. Heparinase 1 selectivity for the 3,6-di-O-sulfo-2-deoxy-2-sulfamido- $\alpha$ -D-glucopyranose (1,4) 2-O-sulfo- $\alpha$ -L-idopyranosyluronic acid (GlcNS3S6S-IdoA2S) linkage. *Glycobiology.* 2011; 21:13–22. [PubMed: 20729345]
16. Fu L, Li G, Yang B, Onishi A, Li L, Sun P, Zhang F, Linhardt RJ. Structural characterization of pharmaceutical heparins prepared from different animal tissues. *J Pharm Sci.* 2013; 102:1447–1457. [PubMed: 23526651]
17. Zhang F, Yang B, Ly M, Solakyildirim K, Xiao Z, Wang Z, Beaudet JM, Torelli AY, Dordick JS, Linhardt RJ. Structural characterization of heparins from different commercial sources. *Anal Bioanal Chem.* 2011; 401:2793–2803. [PubMed: 21931955]

18. Linhardt RJ, Rice KG, Kim YS, Lohse DL, Wang HM, Loganathan D. Mapping and quantification of the major oligosaccharide components of heparin. *Biochem J.* 1988; 254:781–787. [PubMed: 3196292]
19. Zhang Z, Xie J, Liu H, Liu J, Linhardt RJ. Quantification of heparan sulfate and heparin disaccharides using ion pairing, reverse-phase, micro-flow, high performance liquid chromatography coupled with electrospray ionization trap mass spectrometry. *Anal Chem.* 2009; 81:4349–4355. [PubMed: 19402671]
20. Mazák K, Beecher CN, Kraszni M, Larive CK. The interaction of enoxaparin and fondaparinux with calcium. *Carbohydr Res.* 2014; 384:13–19.
21. Achour O, Bridiau N, Godhmani A, Joubioux FL, Juchereau SB, Sannier F, Piot JM, Arnaudin IF, Maugard T. Ultrasonic-assisted preparation of a low molecular weight heparin (LMWH) with anticoagulant activity. *Carbohydr Polym.* 2013; 97:1737–1743.
22. Chen J, Jones CL, Liu J. Using an enzymatic combinatorial approach to identify anticoagulant heparansulfate structures. *Chem Biol.* 2007; 14:986–993. [PubMed: 17884631]
23. Edens RF, Al-Hakim A, Weiler JM, Rethwisch DG, Fareed J, Linhardt RJ. Graduate polyacrylamide gel electrophoresis for detemuration of the molecular weights of heparin derivatives. *J Pharm Sci.* 1992; 81:823–827. [PubMed: 1328601]
24. Pervin A, Gallo C, Jandik KA, Han X-J, Linhardt RJ. Preparation and structural characterization of large heparin-derived oligosaccharides. *Glycobiology.* 1995; 5:83–95. [PubMed: 7772871]
25. Bitter T, Muir HM. A modified uronic acid carbazole reaction. *Anal Biochem.* 1962; 4:330–334. [PubMed: 13971270]
26. Guerrini M, Guglieri M, Naggi A, Sasisekharan R, Torri G. Low molecular weight heparins: structural differentiation by bidimensional nuclear magnetic resonance spectroscopy. *Semin Thromb Hemost.* 2007; 33:478–487. [PubMed: 17629844]
27. Wu J, Zhang C, Mei X, Li Y, Xing XH. Controllable production of low molecular weight heparins by combinations of heparinase I/II/III. *Carbohydr Polym.* 2014; 101:484–492.
28. Mikhailov D, Young HC, Linhardt RJ, Mayo KH. Heparin Dodecasaccharide Binding to Platelet Factor-4 and Growth-Related Protein- $\alpha$ : Introduction of a Partially Folded State and Implications for Heparin Induced Thrombocytopenia. *Journal of Biological Chemistry.* 1999; 274:25317–25329. [PubMed: 10464257]

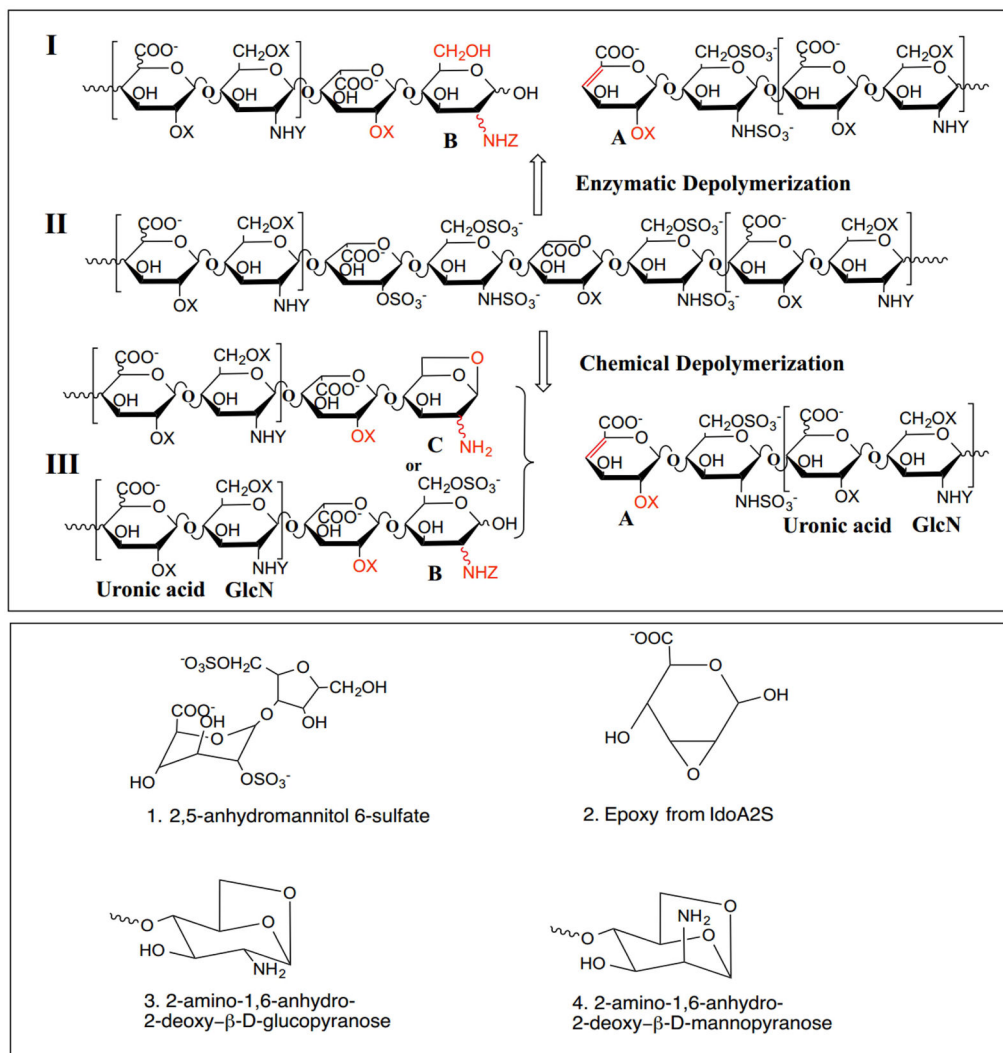


**Figure 1.**

Structural features and process artifacts in LMWHs. Upper panel: Major structures of a LMWH prepared using heparin lyase I, Tinzaparin (**I**), UFH from porcine intestine (**II**) and commercial LMWH, Enoxaparin (**III**). (X= SO<sub>3</sub><sup>-</sup> or H; Y=SO<sub>3</sub><sup>-</sup> or Ac<sup>-</sup>; Z= SO<sub>3</sub><sup>-</sup>, Ac<sup>-</sup> or H). Lower panel: Process artifacts present in LMWHs prepared using chemical processes.

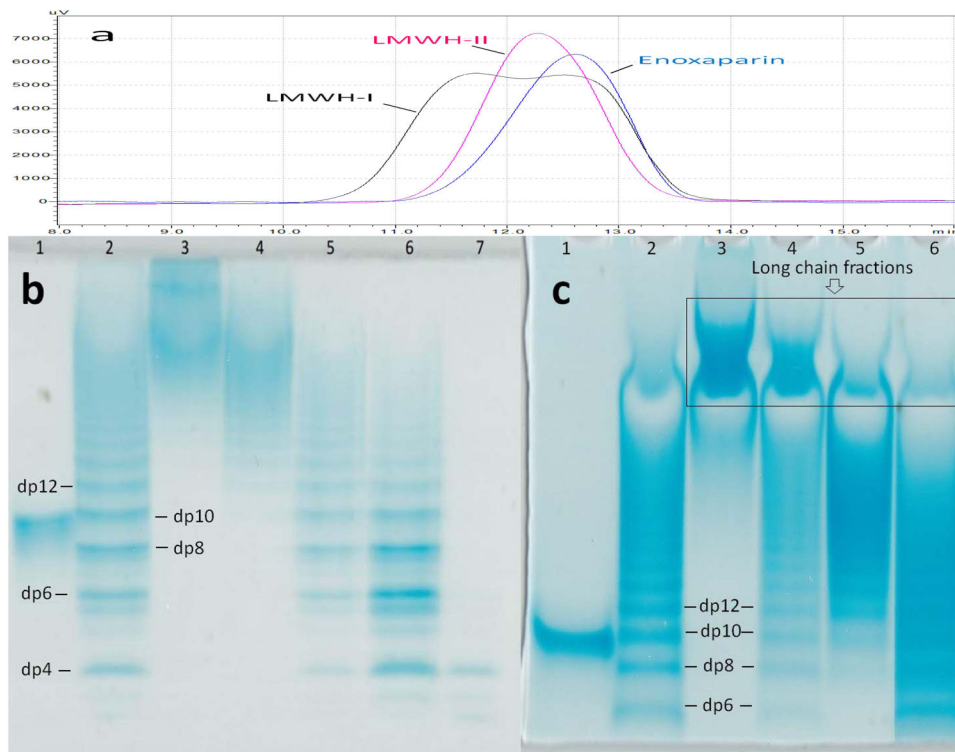


**Figure 2.**

Molecular weight analysis of LMWHs (a) SEC analysis of LMWHs; (b) PAGE analysis of heparin oligomers trapped on the different MWCO membranes: Lane 1, dp10; Lane 2, partially digested bovine lung heparin ladder; Lane 3, 30KT; Lane 4, 10KT; Lane 5, 5KT; Lane 6, 3KT; Lane 7, 3KP.(c)PAGE analysis of LMWHs: Lane 1, dp10; Lane 2, partially digested bovine lung heparin ladder; Lane 3, UFH; Lane 4, LMWH-I; Lane 5, LMWH-II; Lane 6, enoxaparin.

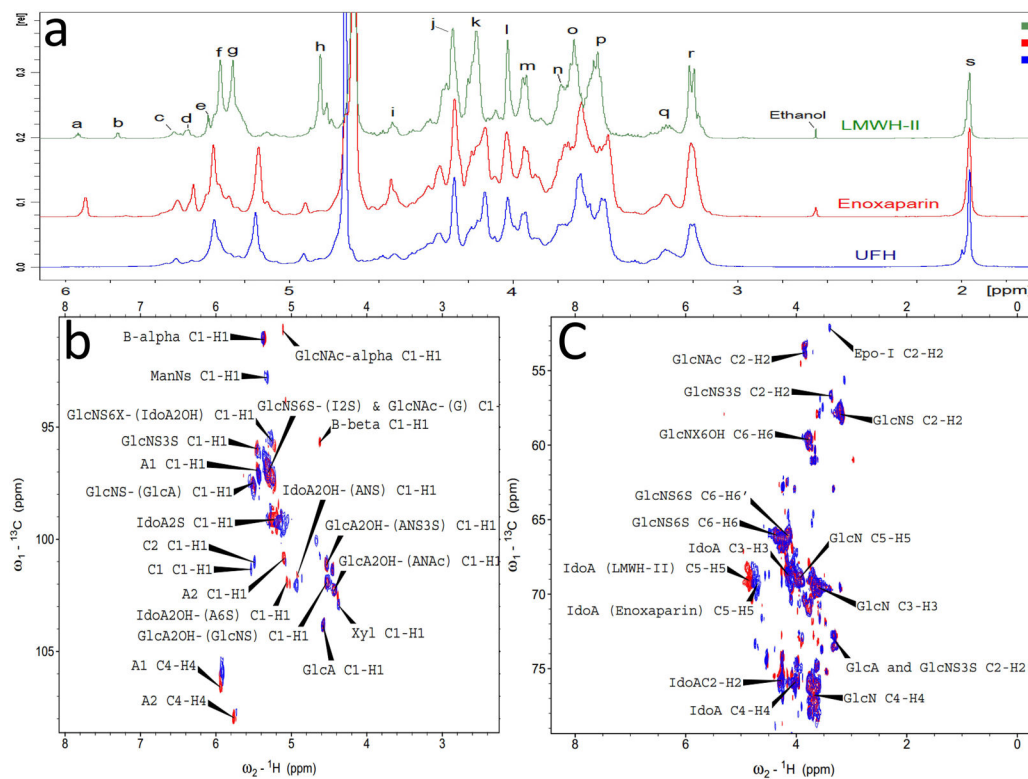


**Figure 3.**

1D  $^1\text{H}$ -NMR and 2D HSQC spectra of heparins. Panel **a**: Comparison and assignments for UFH, enoxaparin and LMWH-II. a, H4 UA<sub>2</sub>S; b, UA<sub>2</sub>OH; c, H1 ANS<sub>6</sub>X-(G); d, H1 ANS<sub>3</sub>S; e, B molecule of  $\alpha$  configuration in panel I and III of Fig. 1; f, H1 ANS<sub>6</sub>X-(I<sub>2</sub>S) and ANAc<sub>6</sub>X-(G); g, H1 I<sub>2</sub>S; h, H5 I<sub>2</sub>S; i, H1 G; j, H2 I<sub>2</sub>S; k, H3 I<sub>2</sub>S; l, H4 I<sub>2</sub>S; m, H5 ANS<sub>6</sub>S; n, H6 ANS; o, H4 ANS<sub>6</sub>S; p, H3 ANS<sub>6</sub>X; q, H2 G and A<sub>3</sub>S,<sub>3</sub>SNS; r, H2 ANS<sub>6</sub>X; s, acetyl CH<sub>3</sub> (A, glucosamine; I, iduronic acid; G, glucuronic acid). Panel **b**: Anomeric region comparison and assignments for LMWH-II (red) and enoxaparin (blue). A1 and A2, UA<sub>2</sub>OH and UA<sub>2</sub>OH, two types of A molecules in panel I and III of Fig. 1; B-alpha and B-beta, B molecules of  $\alpha$  and  $\beta$  configurations in panel I and III of Fig. 1; C1 (Fig. 1 Panel 3) and C2 (Fig. 1 Panel 4), C molecules in Fig. 1 Panel III; Panel **c**: Aliphatic region comparison and assignments for LMWH-II (red) and enoxaparin (blue). Epo-I, epoxide formed from the alkaline treatment of I<sub>2</sub>S (Fig. 1 Panel 2). Selected signals were labeled based on the assignments of Guerrini *et al*<sup>25</sup>.

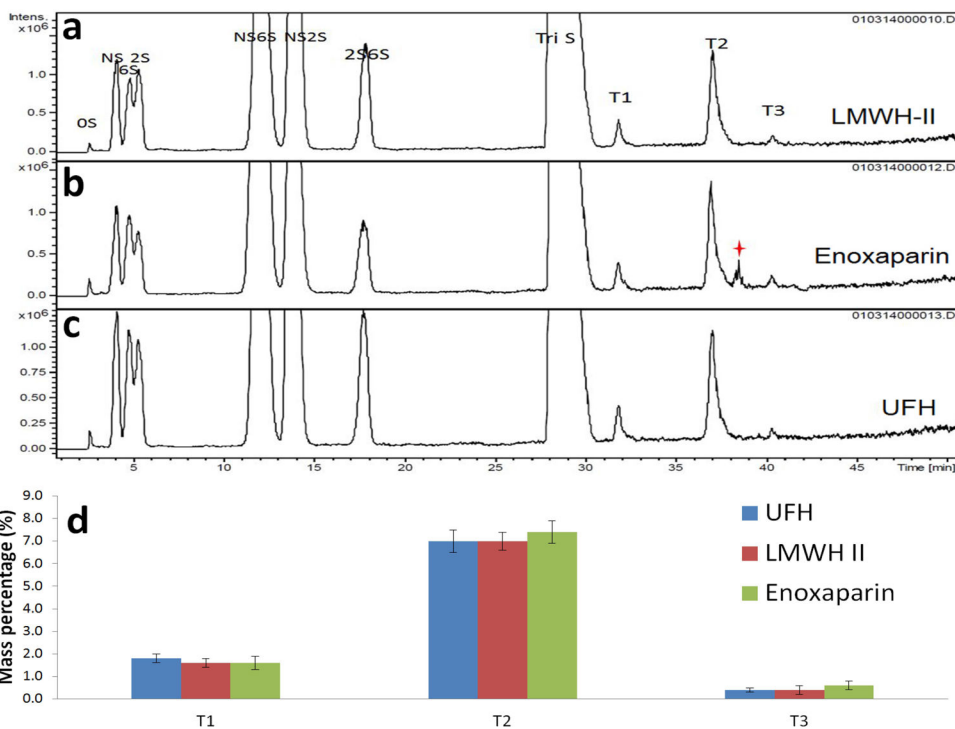


**Figure 4.**

Tetrasaccharide mapping data for LMWH-II, enoxaparin and UFH. Extracted ion chromatography (EIC) of LMWH-II (a), enoxaparin (b) and UFH (c). The star indicates unidentified tetrasaccharide peak. (d) The relative mass percentages of the heparin lyase II-resistant tetrasaccharides. T1, UA-GlcNAc6S-GlcA-GlcNS3S; T2, UA-GlcNAc6S-GlcA-GlcNS3S6S; T3, UA-GlcNS6S-GlcA-GlcNS3S6S

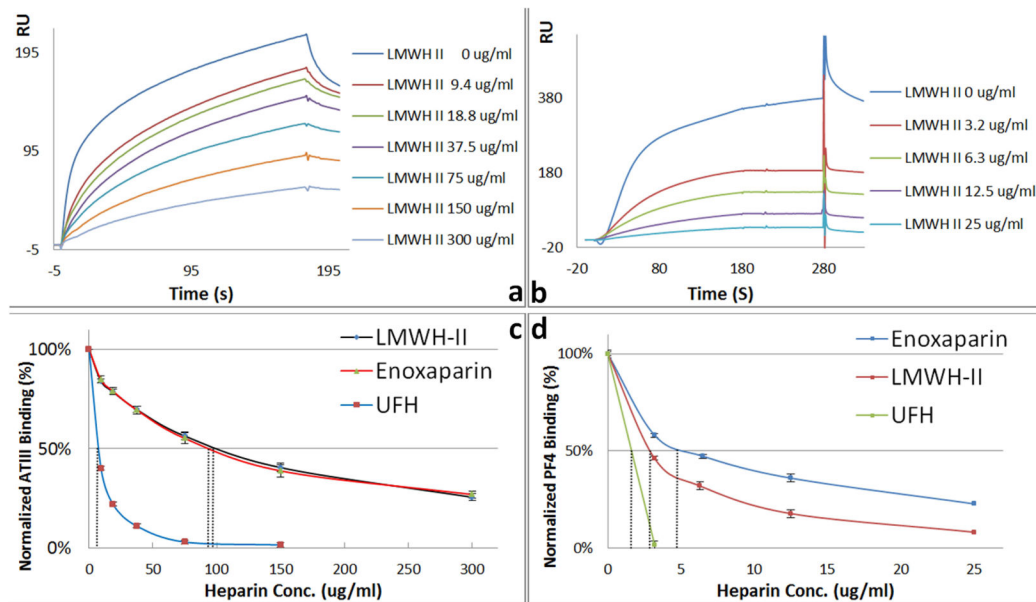


**Figure 5.**

Surface plasmon resonance (SPR) sensorgrams and IC<sub>50</sub> measurement of LMWH-II, enoxaparin and UFH using surface competition SPR. (a) Competition SPR sensorgrams of ATIII-heparin interaction (solution LMWH/surface heparin competition); (b) Competition SPR sensorgrams of PF4-heparin interaction (solution LMWH/surface heparin competition); (c) IC<sub>50</sub> measurement for ATIII binding; (d) IC<sub>50</sub> measurement for PF4 binding.



**Table 1**

Permeation ratio of purified heparin oligomers by membranes.

Membrane pore size	Oligosaccharide permeation percentages (%)		
	dp8	dp10	dp12
3-KDa	15.6%	6.4%	3.5%
5-KDa	29.5%	23.3%	7.6%
10-KDa	61.7%	53.4%	47.4%

**Table 2**

Different reactions and products of enzymatic ultrafiltration

Reaction	Products	Enzyme	N <sub>2</sub> Pressure (psi)	Yield (%)
R1		Heparin lyase I, 120 mU	2	30.5
R2		Heparin lyase I, 250 mU	2	38.2
<b>R3</b>	<b>LMWH-I</b>	<b>Heparin lyase I, 250 mU</b>	<b>20</b>	<b>80.1</b>
R4		Heparin lyase II, 120 mU	2	20.8
R5		Heparin lyase II, 250 mU	2	35.7
<b>R6</b>	<b>LMWH-II</b>	<b>Heparin lyase II, 250 mU</b>	<b>20</b>	<b>81.6</b>

**Table 3**

Average molecular weight of heparins using SEC.

Sample	$M_N$	$M_w$	$M_w/M_N$
UFH	$14618 \pm 114$	$24899 \pm 244$	1.7
LMWH-I	$5500 \pm 30$	$8560 \pm 80$	1.6
LMWH-II	$5090 \pm 50$	$6250 \pm 60$	1.2
Enoxaparin	$3190 \pm 20$	$4215 \pm 30$	1.3
Enoxaparin*	$4372 \pm 231$	$5629 \pm 233$	1.3
Dalteparin*	$5835 \pm 271$	$6626 \pm 222$	1.1
Tinzaparin*	$5833 \pm 223$	$7333 \pm 155$	1.2

\* Data based on the results from Achour O.*et al.*<sup>21</sup>

Table 4

HS/HP disaccharide composition analysis by LC-MS.

Samples	HS/HP disaccharides composition (%)									
	Di-0S	Di-1S	Di-6S	Di-2S	Di-NS6S	Di-NS2S	Di-2S6S	Di-Tris		
UFH	0.8 ± 0.2	1.9 ± 0.1	2.4 ± 0.5	1.4 ± 0.5	14.1 ± 0.8	5.4 ± 0.2	1.5 ± 0.2	72.6 ± 0.3		
LMWH-II	0.6 ± 0.3	1.8 ± 0.3	<b>1.9 ± 0.5</b>	1.6 ± 0.4	<b>10.5 ± 0.7</b>	5.3 ± 0.3	1.6 ± 0.2	<b>76.8 ± 0.1</b>		
Enoxaparin	0.6 ± 0.5	1.8 ± 0.5	2.2 ± 0.8	1.1 ± 0.4	15.2 ± 0.9	4.3 ± 0.4	1.7 ± 0.3	73.1 ± 0.2		

\* Data shown in bold indicate significant compositional differences between LMWH-II and UFH and Enoxaparin.

**Table 5**

Composition and molecular mass of tetrasaccharides formed in mapping experiment

Fractions	m/z	Calculated Mol Mass	Theoretical Mol Mass	Sequence
<b>T1</b>	[477.4] <sup>2-</sup>	956.8	956.1	UA-GlcNAc6S-GlcA-GlcNS3S
<b>T2</b>	[517.4] <sup>2-</sup>	1036.8	1036	UA-GlcNAc6S-GlcA-GlcNS3S6S
<b>T3</b>	[536.3] <sup>2-</sup>	1074.6	1074	UA-GlcNS6S-GlcA-GlcNS3S6S

**Table 6**

Anti-Xa and anti-IIa activity of UFH, LMWH-II and commercial LMWHs.

Heparin	Anti-Xa activity (U/mg)	Anti-IIa activity (u/mg)	Anti-Xa/anti-IIa (ratio)
<b>UFH</b>	201	201	1
<b>LMWH-II</b>	163 ± 4	59 ± 6	2.7
<b>Enoxaparin</b>	170 ± 5	47 ± 4	3.6
<b>Enoxaparin</b> *	184 ± 2	45 ± 3	4.1
<b>Nadroparin</b> *	178 ± 9	67 ± 4	2.7
<b>Dalteparin</b> *	172 ± 6	93 ± 9	2.4
<b>Tinzaparin</b> *	181 ± 7	45 ± 3	3.9

\* Data based on the results from Achour O. *et al.*<sup>21</sup>